Journal of Molecular Science

Journal of Molecular Science
Volume 36 Issue 2, Year of Publication 2026, Page 647-660
DoI-10.004687/1000-9035.2026.075

Journal of Molecular Science
www.jmolecularsci.com ISSN:1000-9035

Formulation, Characterization, and Evaluation of Erlotinib Hydrochloride-Loaded Maltodextrin-Based Proniosomal Tablets

Raghunath S. Sakhare, *Dr. Ram S. Sakhare, Dr. Avinash R. Tekade**
Centre for Research in Pharmaceutical Sciences (CRPS), Channabasweshwar Pharmacy College (Degree), Latur-413512, Maharashtra, India.

Article Information
Received: 13-06-2026
Revised: 21-06-2026
Accepted: 12-07-2026
Published: 29-07-2026

Keywords
Erlotinib hydrochloride, Proniosomes, Box–Behnken Design, Drug delivery system, Controlled release, anticancer therapy.

ABSTRACT
Objective: The objective of the present study was to develop and optimize Erlotinib hydrochloride-loaded proniosomal tablets to enhance drug solubility, oral bioavailability, and therapeutic efficacy through sustained drug release using a Quality by Design (QbD) approach. **Methods:** Proniosomes were prepared by the slurry method using Span-60, cholesterol, and maltodextrin, and optimized using Box–Behnken Design. The formulations were evaluated for drug content, entrapment efficiency, particle size, PDI, zeta potential, SEM, and *in vitro* drug release. The optimized proniosomes were compressed into tablets and evaluated for pre and post-compression parameters, dissolution, and accelerated stability. Pharmacodynamic evaluation was performed in a VX2 liver tumor rabbit model by assessing tumor progression, survival, hematological, biochemical, and histopathological parameters. **Results:** The optimized Proniosomal formulation (ER2) exhibited drug content of 95.96 ± 0.12%, entrapment efficiency of 94.64 ± 0.05%, particle size of 188.4 nm, and zeta potential of −25.3 mV. The optimized tablet formulation (ET7) demonstrated acceptable Pharmaceutical characteristics, drug content of 95.59 ± 0.00%, and sustained drug release of 97.38 ± 0.03% over 24 h. Furthermore, the formulation remained stable under accelerated storage conditions. *In vivo* pharmacodynamics evaluation revealed significant suppression of tumor growth, prolonged survival, improvement in hematological and biochemical indices, and reduced systemic toxicity compared with the tumor control group. **Conclusion:** The optimized Erlotinib hydrochloride-loaded proniosomal tablet exhibited desirable physicochemical properties, sustained drug-release behavior, and good stability. In the VX2 liver tumor rabbit model, the formulation demonstrated notable anticancer activity, characterized by suppression of tumor growth, prolonged survival, improvement in hematological and biochemical parameters, and reduced systemic toxicity. The findings indicate that proniosomal tablet formulation may provide an effective approach for the oral delivery of Erlotinib hydrochloride and contribute to improved therapeutic outcomes.

1. INTRODUCTION:

With a devastating impact on people of all ages, genders, and ethnicities, cancer continues to rank as one of the world's top health concerns and the second worst killer [1]. Even though chemotherapy has come a long way, traditional anticancer treatments still have their drawbacks. These include low selectivity, systemic toxicity, and the difficulty to keep the drug concentration at the target site at an appropriate level. Researchers in the pharmaceutical industry have responded to these difficulties by concentrating on creating new drug delivery methods that may increase therapeutic effectiveness

Journal of Molecular Science
Volume 36 Issue 2, Year of Publication 2026, Page 647-660
DoI-10.004687/1000-9035.2026.075

while decreasing side effects [2].

Biodegradable and biocompatible polymer-based drug delivery technologies have received a lot of attention as of late. Targeted delivery to certain tissues or cells is another goal of modern systems that aim to offer regulated and prolonged medication release. Unfortunately, physiological needs are still unmet by many traditional controlled-release devices. Therefore, there is an increasing need for the creation of sophisticated delivery systems that can monitor physiological signals and adjust medication release appropriately [3,4].

The use of vesicular systems and colloidal particle carriers including ethosomes, transferosomes, niosomes, and liposomes has shown to be far more advantageous than the use of ordinary dosage forms. By modifying their composition or surface features, these systems may encapsulate hydrophilic and hydrophobic medicines, serve as drug reservoirs, and modify the release characteristics. Aggregation, fusion, leakage, hydrolysis, and oxidation are stability concerns that restrict the practical applicability of aqueous vesicular dispersions [7,8].

The idea of provesicular systems was devised to circumvent these restrictions. Niosomal dispersions may be formed by hydrating proniosomes, which are dry, free-flowing formulations made of carriers covered with surfactants [9,10]. The systems avoid problems including aggregation, sedimentation, and leakage, which improves their physical and chemical stability compared to ordinary niosomes. Unit dose forms, including capsules and tablets, may be readily prepared from promiosomes, which improves patient compliance and makes administration more convenient[11,12].

Oral bioavailability and drug penetration across biological membranes are two areas where proniosomal technologies show promise [13]. When they are hydrated, they may encapsulate medications and release them in a regulated and sustained manner because they form multilamellar vesicles. Furthermore, macrophage phagocytosis of these vesicles may enhance medication targeting, especially in cancer treatment [14,15].

Cancers of the pancreas and non-small cell lung may be treated with erlotinib hydrochloride, a drug that inhibits the tyrosine kinase activity of the epidermal growth factor receptor (EGFR). But it has limited clinical use due to issues such low oral bioavailability, poor aqueous solubility, and the need to maintain therapeutic plasma concentrations [16,17,18]. On top of that, its therapeutic effectiveness is often linked to toxicity that varies with dosage. Consequently, a method of administration is required that may lessen systemic toxicity, increase bioavailability, and provide controlled drug release [19,20].

The current research aims to improve the solubility, permeability, and prolonged drug release of erlotinib by developing proniosomal loaded tablets. This methodology shows promise as a method for anticancer medication administration since it has the potential to enhance the therapeutic efficiency of Erlotinib and increase its bioavailability with minimal side effects.

2. PROCEDURES AND INGREDIENTS

2.1 Supplies

A great donation of erlotinib hydrochloride was made by MSN Laboratories of Hyderabad, India. The Netherlands-based Carbogen Amcis provided the cholesterol. Research Lab Fine Chem Industries Pvt. Ltd. of Mumbai, India, supplied the sorbitan monostearate (Span 60), maltodextrin, chloroform, and ethanol. Crospovidone, lactose monohydrate, and microcrystalline cellulose (MCC) were acquired from Loba Chemie Pvt. Ltd. of Mumbai, India. Our suppliers, SD Fine-Chem Limited of Mumbai, India, supplied the talc and magnesium stearate. Analytical grade chemicals, solvents, and excipients were used throughout the investigation.

1.2 Procedures

1.2.1 Proniosome formation

The slurry process was used to manufacture promniosomes. A chloroform-ethanol (1:1) combination was used to dissolve Span-60 and cholesterol, and then the medication was added. To make a consistent slurry, the combination was first sonicated at 45°C until completely dissolved, and then added to the maltodextrin while being constantly mixed. To eliminate the organic solvents, the mixture was dried in a rotary evaporator at 49 ± 2 °C while subjected to decreased pressure. After a further 24 hours of drying in a desiccator, the recovered proniosomal powder was placed in airtight containers until it was ready for further assessment and characterization [21].

Research Methodology

Utilizing a three-factor, three-level Box-Behnken Design (BBD) and Response Surface Methodology (RSM), the proniosomal formulation was optimized with a minimal number of experimental runs utilizing a Quality by Design (QbD) method. The following were chosen as independent variables: Span-60 (A), cholesterol (B), and maltodextrin (C). The response variables were drug content (Y_1), entrapment efficiency (Y_2), and particle size (Y_3). Table 1 displays the results of the low, medium, and high levels of evaluation for the variables.

Journal of Molecular Science
Journal of Molecular Science
Volume 36 Issue 2, Year of Publication 2026, Page 647-660
DoI-10.004687/1000-9035.2026.075

Table 1: Box-Behnken Design's Dependent and Independent Variables

Independent variables	Low value(-1)	Medium (0)	High value(+1)
Span-60 (mg) (A)	80	90	100
Cholesterol (mg) (B)	100	150	200
Maltodextrin (mg) (C)	100	150	200
Dependent variables	Constraints		
Drug Content (%)	Maximize		
Entrapment efficiency (%)	Maximize		
Particle Size (nm)	Minimize		

Table 2: Experimental batch proposed by DOE

Formulation code	Erlotinib (mg)	Span-60 (mg)	Cholesterol (mg)	Maltodextrin (mg)
ER1	25	90	200	100
ER2	25	90	150	150
ER3	25	90	150	150
ER4	25	100	150	200
ER5	25	100	150	100
ER6	25	100	200	150
ER7	25	100	100	150
ER8	25	80	150	100
ER9	25	90	100	100
ER10	25	80	150	200
ER11	25	90	200	200
ER12	25	80	200	150
ER13	25	80	100	150

1.2.1 FORMULATION OF ERLOTINIB PRONIOSOMAL TABLETS

The optimized proniosomal powder was blended with microcrystalline cellulose (MCC), crospovidone, lactose, talc, and magnesium stearate after passing through a 60-mesh sieve. The lubricated blend was directly compressed into tablets using a rotary tablet compression machine and stored in airtight containers until further evaluation [22].

Experimental Design

Optimizing the tablet formulation was done using a Quality by Design (QbD) technique that used Response Surface Methodology (RSM) and a three-factor, three-level Box-Behnken Design (BBD). Y_1 for friability, Y_2 for drug content, and Y_3 for cumulative drug release were the response variables, whereas MCC (A), crospovidone (B), and magnesium stearate (C) were the independent variables. Table 3 displays the results of the three levels of analysis for the variables.

Table 3: Box-Behnken Design's Dependent and Independent Variables

Independent variables	Low value(-1)	Medium (0)	High value(+)
MCC (mg) (A)	40	50	60
Crospovidone (mg) (B)	5	10	15
Magnesium stearate (mg) (C)	3	5	7
Dependent variables	Constraints		
Friability (%)	Minimize		
Drug content (%)	Maximize		
% Drug release (%)	Maximize		

Table 4: Formulation Table of tablet containing Erlotinib Proniosomes

Batch	ER (mg)	MCC (mg)	Crospovidone (mg)	Magnesium Stearate (mg)	Talc (mg)	Lactose (mg)
ET 1	415.12	40	5	5	2.5	14.38
ET 2	415.12	50	15	3	2.5	17.38
ET 3	415.12	40	10	3	2.5	20.38
ET 4	415.12	40	10	7	2.5	24.38
ET 5	415.12	60	10	3	2.5	19.38
ET 6	415.12	50	15	7	2.5	32.38
ET 7	415.12	50	10	5	2.5	22.38
ET 8	415.12	50	5	3	2.5	12.38
ET 9	415.12	60	15	5	2.5	9.38
ET 10	415.12	60	5	5	2.5	2.38
ET 11	415.12	40	15	5	2.5	10.38
ET 12	415.12	60	10	7	2.5	25.38
ET 13	415.12	50	5	7	2.5	5.38

2. EVALUATIONS OF PRONIOSOMES

3.1 Yield Percentage

The preparation procedure was evaluated by calculating the percentage yield of proniosomal formulations loaded with Erlotinib. Weighing the powder after it had dried at 40-50°C, we were able to determine its percent yield by dividing its actual yield by its theoretical yield [23].

$$(\%)\ \textbf{yield} = \frac{\text{Practical Yield}}{\text{Therotical yield}} \times 100 \quad \text{…….. (1)}$$

3.2 Drug content

Erlotinib -loaded proniosomes (20 mg) were extracted with methanol (10 mL) for 10 mins, and percent drug loading was calculated by taking UV absorbance [24].

$$(\%)\text{Drug content} = \frac{\text{Amount of drug in formulation}}{\text{Qty of formulation used}} \times 100\text{…….. (2)}$$

3.3 Entrapment efficiency

Entrapment efficiency was determined by

Journal of Molecular Science
Journal of Molecular Science
Volume 36 Issue 2, Year of Publication 2026, Page 647-660
DoI-10.004687/1000-9035.2026.075

measuring unentrapped drug in the supernatant. The dispersion (1 mL) was centrifuged at 17,000 rpm for 30 min, and the supernatant was analyzed spectrophotometrically at its wavelength. Entrapped drug was calculated by subtracting free drug from the total, and EE % was determined using the following equation [25].

$$\textit{Entrapment efficiency}(\%) = \frac{\textit{Added drug} - \textit{Free drug}}{\textit{Added}} \times 100 \ldots\ldots\ldots (3)$$

3.4 Particle size

Dynamic light scattering (HORIBA, SZ-100V2) was used in triplicate at 25°C and a 90° scattering angle to evaluate the particle size of proniosomes. The intensity profile was used for data analysis after samples were diluted 1:100 with Milli-Q water [26].

3.5 Drug Diffusion in a Vitro

The proniosomal formulation containing Erlotinib was subjected to an in vitro drug diffusion analysis utilizing a Franz diffusion cell. Sodium phosphate buffer saline (PBS, pH 7.4) was used to soak a dialysis membrane before it was installed between the donor and receptor compartments. To guaranty that the dispersed active was evenly distributed, the receptor compartment was filled with PBS (pH 7.4) and kept at 37 ± 0.5°C with continuous magnetic stirring. The donor compartment was filled with a precisely determined amount of the proniosomal formulation that was equal to a known amount of active. A 1 mL sample was removed from the receptor compartment and replaced with a fresh 1 mL amount of PBS kept at the same temperature at regular intervals. A UV spectrophotometer was used for the analysis of the gathered samples. Through the use of the UV calibration equation, the cumulative percentage of drug diffusion was computed [28].

3.6 SEM

The surface morphology of the improved Proniosome batch was examined using scanning electron microscopy. In order to evaluate the surface topography, texture, and fracture morphology, pictures were taken at a magnification of 500×.

3. Evaluations Of Proniosomes Containing Tablet

4.1 Evaluation of Precompression Blend:

The powder blend's flowability and compressibility were assessed by measuring its bulk density, tapped density, angle of repose, Carr's compressibility index, and Hausner's ratio before compression. We found the angle of repose by plugging the powder cone's height (H) and its base radius (R) into the formula $\Theta = \tan^{-1}(H/R)$. The mass of the powder (M), the bulk volume (Vb), and the tapped volume (Vt) were used to determine the bulk density (Bulk Density = M/Vb) and the tapped density (Tapped Density = M/Vt), respectively.

The flow properties of the blend were further evaluated by calculating Carr's compressibility index [(Tapped Density − Bulk Density)/Tapped Density] × 100 and Hausner's ratio (Tapped Density/Bulk Density) according to the reported methods [22,29].

4.2 Post Compression Parameters

i. Weight variation

We compared the weights of each pill to the average weight after randomly weighing twenty of them. No more than one pill could be found to be beyond the specified range while checking for weight variation [30].

ii. Average thickness

The vernier caliper was used to measure the tablet thickness. The tablet thickness would fall within a ±5% range of the mean value, as stated in the report.

iii. Hardness

The Monsanto Hardness Tester was used to determine the tablet hardness for each formulation.

iv. iv. Friability

Using a Roche Friabilator, we were able to assess the tablet's friability. The friabilator was turned on at 25 revolutions per minute for four minutes after ten pills were weighed and put in. After that, the pills were removed, dried, and then weighed again. The formula was used to determine the percentage of tablet friability:

$$\text{Percentage friability} = \frac{\text{Initial weight} - \text{final weight}}{\text{Initial weight}} \times 100 \ldots\ldots\ldots (9)$$

v. Wetting Time

A tablet was put on the surface of a band of filter paper mounted on a glass slide, and a glass Petri dish was half filled with a 0.1% methylene blue solution in water. The tablet's bottom surface was where the 0.1% methylene blue solution was absorbed. Time necessary for dye solution to reach the center of top surface of tablet was reported as wetting time [30].

Time of Disintegration::

Disintegration test equipment was used to conduct the disintegration test. Each tube contains one tablet, and the basket rack is put in a 1-liter beaker filled with 0.1 N HCL at 37°C ±2°C. The basket assembly holding the tablets is moved up and down a distance of 5 to 6 cm at a frequency of 28 to 32 cycles per minute using a typical motor-driven device. It was noticed how long it took for the pill to totally dissolve [30].

Drug content

One tablet's worth of powdered tablets were dissolved in pH 6.8 phosphate buffer, filtered, and suitably diluted. UV spectroscopy was used to detect absorbance, and a standard curve was used to determine the drug concentration. The process was carried out three times, and the mean ± SD was used to represent the findings.

Journal of Molecular Science
Volume 36 Issue 2, Year of Publication 2026, Page 647-660
DoI-10.004687/1000-9035.2026.075

***In vitro* Dissolution Studies:**
USP dissolving equipment II was used to study in vitro drug release in 900 mL pH 6.8 buffer at 37 ± 0.5 °C and 100 rpm for 60 hours. At 0.5, 1, 2, 3, 4, 6, 8, 10, 12, 14, 16, 18, 20, 22, and 24 hours, samples (5 mL) were removed, replaced with new medium, filtered (0.45 µm), diluted, and examined. The percentage of cumulative medication release was computed [31].

Analysis of stability study
In accordance with ICH standards (ICH Q1A-R2) on optimal formulation, the expedited stability tests were conducted. For three months, the formulation was kept in a stability chamber at 40 °C and 75% relative humidity after being wrapped in an aluminum foil strip. The tablet's friability, drug content, and in vitro drug release were assessed both before and after three months [32].

4. *In vivo* Studies
5.1 Test Animals
For the investigation, healthy adult male New Zealand White rabbits weighing between 2.5 and 3.5 kg were employed. The animals were kept in hygienic polypropylene cages with room temperature (22 ± 2°C), relative humidity (55 ± 5%), and a 12-hour light/dark cycle. The Institutional Animal Ethics Committee (IAEC) authorized protocol no. IRDA/IAEC/M05/96/2025-26, which gave them unrestricted access to clean water and a regular pellet diet.

Table 5: Experimental Grouping

Group	Treatment
I	Normal control (vehicle only)
II	Tumor control (untreated)
III	Tumor + ET-7 (low dose)
IV	Tumor + ET-7 (high dose)
V	Tumor + Standard anticancer drug (Erlotinib 25mg)

5.2 New Zealand White rabbit VX2 Liver Tumor Model.
For the implantation of VX2 liver tumors, male New Zealand White rabbits weighing between 2.5 and 3.5 kg were kept in conventional laboratory settings. Donor rabbits were used to extract VX2 tumor tissue, which was then evaluated for viability and cut into 1-2 mm^3 pieces. Ketamine (35 mg/kg) and xylazine (5 mg/kg) were used to anesthetize the rabbits, and the liver was exposed either a midline or subcostal laparotomy. A single tumor fragment was inserted into the left or medial hepatic lobe, sealed with tissue adhesive (gelatin sponge), and the abdomen closed with absorbable sutures. Buprenorphine (0.05 mg/kg) analgesia and wound healing monitoring were part of postoperative treatment.

Therapy given
Tumor development was established by imaging and histology within 7–28 days. During the course of therapy, the regular medication and test proniosomal tablet solutions were given orally once daily [33, 34].

5.3 Sample Collection
Blood samples were taken from rabbits' marginal ear veins at pre-arranged intervals after medication delivery in order to assess pharmacodynamics. To separate plasma, around 1-2 mL of blood was aseptically collected into heparinized tubes and centrifuged for 10 minutes at 3000 rpm. The collected plasma samples were kept at –20 °C for further biochemical and pharmacodynamic examination.

Animals were killed under anesthesia at the conclusion of the research, and tumor tissue and essential organs were taken for histological analysis and pharmacodynamic response assessment [35].

5.4 Parameters for the experiment
Numerous physiological, biochemical, hematological, and histological markers linked to anticancer efficacy were assessed in order to conduct the pharmacodynamic investigation. Throughout the trial, the animals' body weight, food intake, water consumption, and behavioral changes were tracked to evaluate their overall health and treatment response. Tumor weight at the conclusion of the trial and tumor volume measured on a regular basis were used to gage tumor progression. To assess the test formulation's anticancer capability, the percentage suppression of tumor development was also calculated.

Pharmacodynamic and biochemical analyzes were conducted using blood samples obtained throughout the trial. To ascertain the treatment's systemic impact, hematological parameters such hemoglobin content, total leukocyte count, differential leukocyte count, and red blood cell count were examined. To evaluate organ function and treatment-related toxicity, biochemical measures such as liver function indicators like ALT, AST, ALP, and bilirubin, as well as kidney function markers like serum creatinine and blood urea nitrogen, were assessed.

5.5 Histopathological Analysis
Following animal sacrifice, tumor, liver, kidney, and spleen tissues were collected and preserved for 24 hours in 10% neutral buffered formalin. An automated tissue processor was used to dehydrate fixed tissues using a succession of graded alcohols, clarify them in xylene, and embed them in paraffin wax.

Journal of Molecular Science

Journal of Molecular Science
Volume 36 Issue 2, Year of Publication 2026, Page 647-660
DoI-10.004687/1000-9035.2026.075

Tissues fixed in paraffin were sectioned using a rotary microtome (Leica Microtome, Germany) to a thickness of 4–5 µm. Hematoxylin and eosin (H&E) staining was applied to tissue slices that were mounted on glass slides.

A trinocular research microscope (Olympus BX53 Microscope, Japan) was used for the histological observations. Cellular morphology, necrosis, inflammatory alterations, tissue degradation, and the restoration of normal architecture after therapy were all evaluated under a microscope [36].

5.6 Analysis of Statistics

The mean ± standard error of mean (SEM) was used to represent all experimental results. One-way analysis of variance (ANOVA) was used for statistical analysis, and Tukey's multiple comparison test or another suitable post hoc test was used to compare the various experimental groups. A statistically significant result was defined as $p < 0.05$. Appropriate statistical software was used to perform the statistical analysis.

5. RESULTS AND DISCUSSION:

6.1 Proniosomes

6.1.1 Percent Yield, Drug Content, Entrapment efficiency

Table 6: % yield, Drug Content, Entrapment efficiency

Formulation Code	% Yield	Drug Content (%)	Entrapment efficiency (%)
ER 1	98.31	83.65 ± 0.03	91.57 ± 0.124
ER 2	99.27	95.96 ± 0.12	94.64 ± 0.05
ER 3	97.59	93.43 ± 0.32	90.38 ± 0.63
ER 4	98.73	94.09 ± 0.82	83.47 ± 0.75
ER 5	98.66	91.36 ± 0.01	76.20 ± 0.09
ER 6	97.89	92.04 ± 0.85	65.25 ± 0.04
ER 7	97.66	92.92 ± 0.32	71.57 ± 0.14
ER 8	97.74	92.81 ± 0.45	80.82 ± 0.09
ER 9	98.73	93.92 ± 0.02	79.44 ± 0.63
ER10	97.36	89.61 ± 0.04	82.66 ± 0.48
ER11	98.64	94.75 ± 0.14	80.28 ± 0.04
ER12	97.14	92.82 ± 0.03	69.76 ± 0.09
ER13	97.46	91.04 ± 0.04	70.86 ± 0.48

The drug content (83.65–95.96%), entrapment efficiency (65.25–94.64%), and percentage yield (97.14–99.27%) of all proniosomal formulations were good. ER2 was the best proniosomal formulation for further testing since it had the greatest drug content (95.96 ± 0.12%) and entrapment efficiency (94.64 ± 0.05%) of all the formulations, demonstrating higher drug loading and encapsulation efficiency.

ANOVA for 2FI model
Response 1: Drug Content

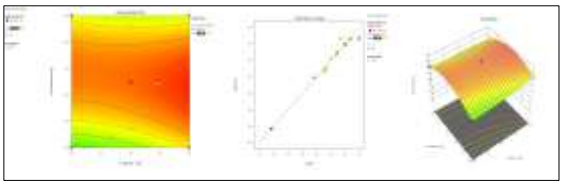

Figure 1: A) Counterplot illustrating how span 60 and cholesterol affect drug content; B) Predicted vs. Actual plot; and C) 3D Surface plot illustrating the same impact

ANOVA for Quadratic model
Response 2: Entrapment efficiency

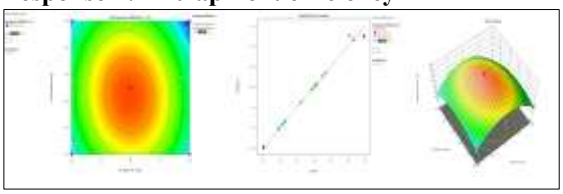

Figure 2: A) Counterplot illustrating how entrapment efficiency is affected by span 60 versus cholesterol B) Predicted vs. Actual plot; C) 3D surface plot illustrating how span 60 and cholesterol affect entrapment efficiency

6.1.2 Particle size

Table 7: Particle size, PDI and Zeta potential

Formulation Code	Particle Size (nm)	PDI	Zeta potential (mV)
ER1	223.2	0.323	-20.4
ER2	188.4	0.219	-25.3
ER3	211.2	0.171	-19.5
ER4	242.4	0.414	-15.2
ER5	334.1	0.165	-21.6
ER6	245.1	0.292	-22.1
ER7	216.4	0.414	-19.5
ER8	312	0.302	-21.3
ER9	265.2	0.185	-15.7
ER10	205.1	0.212	-21.2
ER11	192.1	0.309	-24.2
ER12	195	0.310	-14.7
ER13	211.1	0.195	-18.9

The produced formulations (ER1–ER13) had zeta potential values between −14.7 mV and −25.3 mV, PDI values between 0.165 and 0.414, and particle diameters between 188.4 nm and 334.1 nm. These findings show that the formulations had adequate homogeneity and reasonable stability within the nanoscale. Overall, the system showed appropriate physicochemical properties for further assessment.

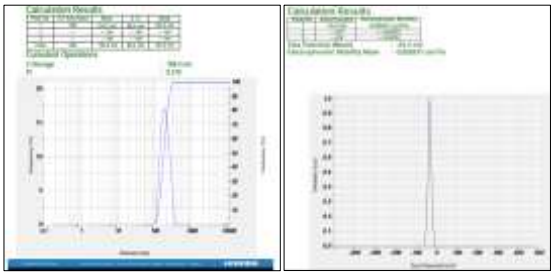

Figure 3: Particle size, PDI and Zeta potential of ER2

Journal of Molecular Science

Journal of Molecular Science
Volume 36 Issue 2, Year of Publication 2026, Page 647-660
DoI-10.004687/1000-9035.2026.075

ANOVA for Linear model
Response 3: Particle Size

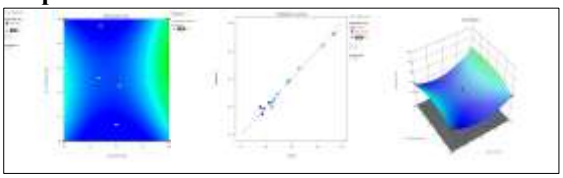

Figure 4: A) Counterplot illustrating how span 60 and cholesterol affect particle size; B) Predicted vs. Actual plot; and C) 3D Surface plot illustrating the same impact

6.1.3 *In Vitro* Drug Release

Table 8: *In vitro* release of ER1 to ER6

Time (Hrs.)	ER1	ER2	ER3	ER4	ER5	ER6
0.5	4.92 ± 0.0054	5.79 ± 0.0061	4.26 ± 0.0048	3.72 ± 0.0052	3.24 ± 0.0041	3.96 ± 0.0047
1	9.99 ± 0.0087	11.07 ± 0.0092	8.85 ± 0.0079	7.83 ± 0.0084	6.93 ± 0.0071	8.22 ± 0.0078
2	15.15 ± 0.0108	16.71 ± 0.0114	13.74 ± 0.0096	12.12 ± 0.0105	10.77 ± 0.0092	12.54 ± 0.0098
3	20.40 ± 0.0127	22.47 ± 0.0133	18.87 ± 0.0115	16.80 ± 0.0124	14.85 ± 0.0109	17.25 ± 0.0118
4	25.71 ± 0.0143	28.29 ± 0.0151	24.36 ± 0.0134	21.66 ± 0.0142	19.20 ± 0.0128	22.14 ± 0.0139
6	31.08 ± 0.0164	34.17 ± 0.0173	30.09 ± 0.0157	26.73 ± 0.0165	23.76 ± 0.0148	27.27 ± 0.0159
8	36.54 ± 0.0188	40.20 ± 0.0196	36.06 ± 0.0181	31.92 ± 0.0189	28.53 ± 0.0172	32.49 ± 0.0184
10	42.12 ± 0.0209	46.38 ± 0.0217	42.09 ± 0.0201	37.29 ± 0.0210	33.42 ± 0.0193	37.89 ± 0.0204
12	47.79 ± 0.0226	52.71 ± 0.0238	48.36 ± 0.0221	42.81 ± 0.0229	38.67 ± 0.0212	43.44 ± 0.0224
14	53.55 ± 0.0247	59.19 ± 0.0259	54.81 ± 0.0243	48.60 ± 0.0252	44.04 ± 0.0235	49.26 ± 0.0246
16	59.37 ± 0.0268	65.85 ± 0.0276	61.38 ± 0.0261	54.54 ± 0.0269	49.68 ± 0.0250	55.26 ± 0.0263
18	65.28 ± 0.0289	72.72 ± 0.0298	68.07 ± 0.0284	60.66 ± 0.0291	55.56 ± 0.0273	61.44 ± 0.0285
20	71.25 ± 0.0312	79.86 ± 0.0325	74.94 ± 0.0307	67.02 ± 0.0316	61.68 ± 0.0298	67.83 ± 0.0309
22	77.34 ± 0.0334	87.18 ± 0.0348	81.93 ± 0.0331	73.65 ± 0.0337	68.34 ± 0.0319	74.55 ± 0.0330
24	83.46 ± 0.0357	93.18 ± 0.0369	89.07 ± 0.0352	80.52 ± 0.0358	76.53 ± 0.0341	81.60 ± 0.0350

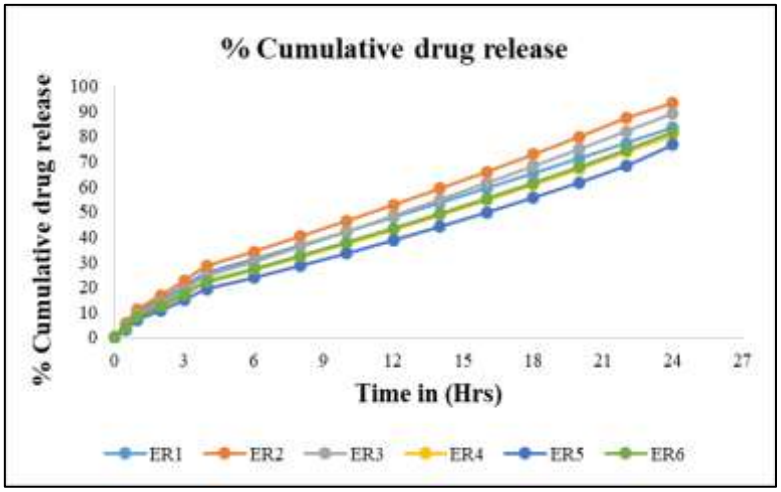

Fig 5: *In vitro* release of ER1 to ER6

Table 9: *In vitro* release of ER7 to ER13

Time (Hrs.)	ER7	ER8	ER9	ER10	ER11	ER12	ER13
0.5	4.38 ± 0.0049	4.59 ± 0.0052	3.93 ± 0.0043	4.32 ± 0.0048	3.78 ± 0.0041	3.39 ± 0.0038	4.47 ± 0.0050
1	9.00 ± 0.0081	9.36 ± 0.0085	8.40 ± 0.0078	8.79 ± 0.0082	7.92 ± 0.0073	7.17 ± 0.0069	9.21 ± 0.0084
2	13.83 ± 0.0105	14.31 ± 0.0111	13.14 ± 0.0102	13.77 ± 0.0108	12.30 ± 0.0096	11.13 ± 0.0091	14.13 ± 0.0110
3	18.81 ± 0.0128	19.38 ± 0.0134	17.97 ± 0.0123	18.99 ± 0.0131	17.04 ± 0.0119	15.27 ± 0.0111	19.20 ± 0.0135
4	23.94 ± 0.0149	24.66 ± 0.0156	23.01 ± 0.0142	24.57 ± 0.0154	22.02 ± 0.0138	19.74 ± 0.0129	24.51 ± 0.0158
6	29.22 ± 0.0173	30.03 ± 0.0181	28.23 ± 0.0169	30.39 ± 0.0185	27.18 ± 0.0164	24.42 ± 0.0152	29.97 ± 0.0182
8	34.71 ± 0.0198	35.64 ± 0.0206	33.66 ± 0.0192	36.48 ± 0.0211	32.46 ± 0.0188	29.31 ± 0.0174	35.61 ± 0.0207
10	40.23 ± 0.0221	41.31 ± 0.0230	39.12 ± 0.0215	42.63 ± 0.0238	37.98 ± 0.0211	34.29 ± 0.0196	41.34 ± 0.0232
12	45.90 ± 0.0243	47.10 ± 0.0252	44.52 ± 0.0237	49.02 ± 0.0264	43.62 ± 0.0234	39.66 ± 0.0219	47.13 ± 0.0254
14	51.78 ± 0.0268	53.07 ± 0.0277	50.34 ± 0.0262	55.56 ± 0.0291	49.50 ± 0.0258	45.18 ± 0.0242	53.07 ± 0.0278
16	57.84 ± 0.0291	59.25 ± 0.0303	56.37 ± 0.0286	62.22 ± 0.0319	55.59 ± 0.0281	50.97 ± 0.0264	59.22 ± 0.0304
18	64.05 ± 0.0315	65.52 ± 0.0328	62.52 ± 0.0310	69.09 ± 0.0346	61.95 ± 0.0305	56.94 ± 0.0288	65.49 ± 0.0329
20	70.47 ± 0.0341	72.03 ± 0.0355	68.88 ± 0.0336	75.99 ± 0.0372	68.43 ± 0.0331	63.21 ± 0.0313	71.97 ± 0.0357
22	77.22 ± 0.0368	78.87 ± 0.0383	75.57 ± 0.0362	82.98 ± 0.0399	75.21 ± 0.0358	70.05 ± 0.0340	78.78 ± 0.0385
24	84.30 ± 0.0394	86.04 ± 0.0411	82.53 ± 0.0389	90.24 ± 0.0427	82.20 ± 0.0382	78.33 ± 0.0365	85.95 ± 0.0413

Journal of Molecular Science

Journal of Molecular Science
Volume 36 Issue 2, Year of Publication 2026, Page 647-660
DoI-10.004687/1000-9035.2026.075

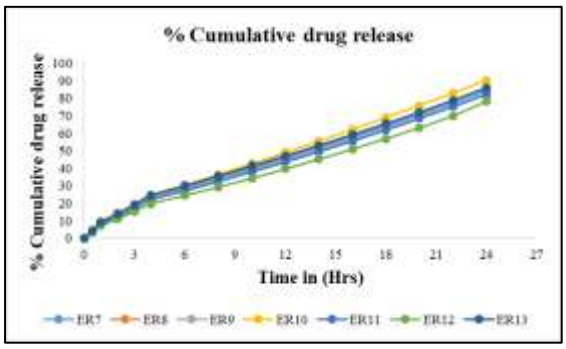

Fig 6: *In vitro* release of ER7 to ER13

For every proniosomal formulation, the in vitro drug release research showed a slow and steady release pattern over a 24-hour period. Among ER1–ER13, drug release varied from 76.53% to 93.18%. At 24 hours, formulation ER2 showed the greatest cumulative drug release (93.18 ± 0.0369%), followed by ER10 (90.24 ± 0.0427%) and ER3 (89.07 ± 0.0352%). Excellent consistency and repeatability of the dissolution results were shown by the low standard deviation values. Because of its better dissolving capability, ER2 was chosen as the optimized proniosomal formulation and overall showed the most effective drug release profile.

6.1.4 SEM

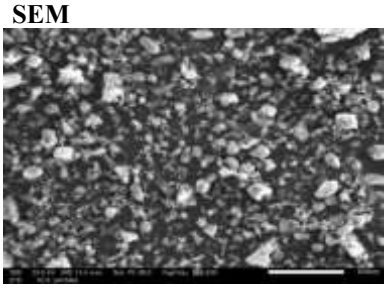

Fig 7: SEM image of ER2

The irregular and heterogeneous particle shape is shown in the 500× magnification SEM picture of ER2. The particles have a wide size variety from sub-microns to several microns, and they seem mostly angular and crystalline. The rough surface roughness suggests a large surface area, which may affect the drug release and dissolving characteristics. There is no discernible aggregation, indicating excellent dispersibility. Overall, the morphology points to ER2's potential for improved homogeneity and solubility in formulation applications.

6.2 Proniosomes Containing Tablet

6.2.1 Pre-compression Blend:

To determine whether formulations ET1–ET13 were suitable for direct compression, their pre-compression properties were examined. The powder mixes' excellent to fair flow qualities were indicated by the angle of repose, which varied from 25.19° to 39.47°. It was discovered that the bulk density and tapped density fell between 0.8024 and 0.9558 g/mL and 0.8025 and 0.9421 g/mL, respectively, indicating satisfactory packing and consolidation behavior.

The blends had excellent to acceptable flowability and compressibility, with Carr's compressibility index values ranging from 5.18% to 23.62% and Hausner's ratio ranging from 1.02 to 1.95. For constant tablet weight throughout compression and homogenous die filling, the measured values show sufficient interparticulate packing and flow characteristics.

Table 10: Angle of repose (ɵ), Bulk Density, Tapped density, Carr's Index, Hausner Ratio

Formulation Code	Angle θ (°)	Flow ability	Bulk Density (g/mL)	Tapped Density (g/mL)	Carr's Index (%)	Hausner Ratio
ET1	25.19	Excellent	0.9015	0.9287 ± 0.0188	15.2523	1.1799
ET2	26.00	Excellent	0.9154	0.9028 ± 0.0125	11.2956	1.1273
ET3	31.27	Good	0.9027	0.9028 ± 0.0125	7.7212	1.0836
ET4	33.68	Good	0.8441	0.8405 ± 0.0062	12.4511	1.1422
ET5	25.51	Excellent	0.9284	0.9244 ± 0.0200	20.4092	1.1708
ET6	39.03	Fair	0.9154	0.8718 ± 0.0413	10.0939	1.1122
ET7	35.39	Good	0.8227	0.8334 ± 0.0107	5.5161	1.0258
ET8	28.99	Excellent	0.8904	0.8312 ± 0.0482	18.9128	1.2332
ET9	32.32	Good	0.8783	0.8312 ± 0.0435	18.7065	1.2301
ET10	36.38	Good	0.9154	0.8721 ± 0.0467	6.5982	1.0706
ET11	31.60	Good	0.9285	0.9335 ± 0.0276	6.6235	1.1024
ET12	35.83	Good	0.9558	0.9421 ± 0.0137	23.6241	1.3093
ET13	39.47	Fair	0.8024	0.8025 ± 0.0100	5.1844	1.9507

6.2.2 Post Compression Parameters

6.2.2.1 Weight variation, Thickness, Tablet Hardness, Friability

Table 11: Weight variation, Thickness, Tablet Hardness, Friability

Formulation code	Weight Variation (%)	Thickness (mm)	Tablet Hardness (kg/cm²)	% Friability
ET 1	0.15	7.40 ± 0.06	4.2 ± 0.2000	0.128
ET 2	0.02	7.46 ± 0.05	4.1 ± 0.1155	0.712

Journal of Molecular Science
Journal of Molecular Science
Volume 36 Issue 2, Year of Publication 2026, Page 647-660
DoI-10.004687/1000-9035.2026.075

ET 3	0.16	7.28 ± 0.04	4.4 ± 0.1528	0.38
ET 4	0.33	7.12 ± 0.05	4.8 ± 0.1155	0.44
ET 5	0.63	7.01 ± 0.04	5.2 ± 0.1528	0.642
ET 6	0.08	6.90 ± 0.05	5.6 ± 0.1528	0.502
ET 7	0.01	6.80 ± 0.04	6.0 ± 0.1000	0.397
ET 8	0.39	6.73 ± 0.03	6.3 ± 0.1155	0.58
ET 9	0.09	6.62 ± 0.04	6.6 ± 0.1155	0.562
ET 10	0.17	6.57 ± 0.05	6.8 ± 0.1000	0.46
ET 11	0.14	6.47 ± 0.04	7.1 ± 0.0577	0.538
ET 12	0.06	7.52 ± 0.06	4.0 ± 0.1528	0.60
ET 13	0.46	7.33 ± 0.05	4.3 ± 0.1155	0.307

With weight variation ranging from 0.01–0.63%, thickness 6.47–7.52 mm, hardness 4.0–7.1 kg/cm², and friability 0.30–0.72% (below 1%), all formulations (ET1–ET13) demonstrated acceptable qualities. These findings show that the tablets have high mechanical stability and homogeneity.

ANOVA for Linear model
Response 1: Friability

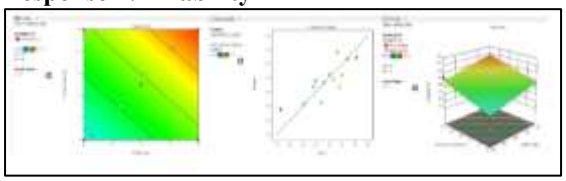

A) B) C)

Figure 8 A) A counterplot comparing the friability of MCC with Crospovidone B) Predicted vs. Actual plot, C) 3D Surface plot comparing the friability of MCC with Crospovidone

6.2.2.2 Wetting Time, Disintegration time, Drug content

Table 12: Wetting Time Disintegration time, Drug content of tablet

Formulation code	Wetting Time (Mins.)	Disintegration time (Mins.)	Drug content (%)
ET 1	33.33 ± 0.5892	6.3 ± 0.0817	75.35 ± 0.0001
ET 2	21.53 ± 0.4046	8.1 ± 0.0817	82.69 ± 0.0036
ET 3	41.33 ± 1.3883	5.2 ± 0.0817	80.49 ± 0.0025
ET 4	51.66 ± 0.6133	6.7 ± 0.0817	91.41 ± 0.0047
ET 5	29.00 ± 0.0001	9.1 ± 0.0817	92.35 ± 0.0084
ET 6	35.33 ± 0.5774	6.9 ± 0.0817	88.83 ± 0.0003
ET 7	45.33 ± 0.5774	7.59 ± 0.0208	95.59 ± 0.0000
ET 8	23.33 ± 0.6589	8.5 ± 0.0817	86.39 ± 0.0009
ET 9	56.66 ± 0.2178	9.1 ± 0.0817	80.98 ± 0.0051
ET 10	31.33 ± 1.5275	7.3 ± 0.0817	84.78 ± 0.0094
ET 11	47.33 ± 0.4131	6.2 ± 0.0817	86.22 ± 0.0027
ET 12	26.33 ± 0.5774	8.4 ± 0.0898	87.77 ± 0.0015
ET 13	54.66 ± 0.7393	7.7 ± 0.0817	76.75 ± 0.0074

With the highest drug content (95.59 ± 0.00%) and appropriate wetting time (45.33 ± 0.58 min) and disintegration time (7.59 ± 0.02 min), ET7 was chosen as the optimum formulation out of all the formulations. This indicated adequate tablet performance and content consistency.

ANOVA for Quadratic model
Response 2: Drug content

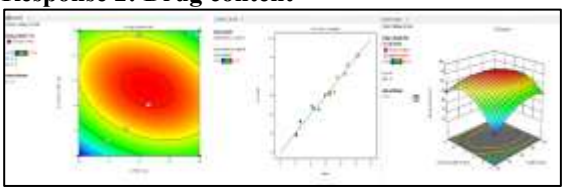

Figure 9: A) MCC vs. Crospovidone on drug content counterplot; B) Predicted vs. Actual plot; and C) MCC vs. Crospovidone on drug content 3D surface plot

6.2.2.3 In vitro Dissolution Studies

Table 13: In vitro drug release of ET 1 to ET6

Time (Hrs.)	ET1	ET2	ET3	ET4	ET5	ET6
0	0	0	0	0	0	0
0.5	3.78 ± 0.0014	4.92 ± 0.0027	4.83 ± 0.0019	5.52 ± 0.0035	5.61 ± 0.0022	5.16 ± 0.0011
1	7.98 ± 0.0028	8.99 ± 0.0041	9.81 ± 0.0033	11.22 ± 0.0052	11.40 ± 0.0037	10.50 ± 0.0024
2	12.45 ± 0.0046	11.15 ± 0.0063	14.88± 0.0051	17.01 ± 0.0070	17.31 ± 0.0058	15.93 ± 0.0042
3	17.13 ± 0.0062	16.40 ± 0.0085	20.04 ± 0.0068	22.89 ± 0.0094	23.31 ± 0.0079	21.45 ± 0.0057
4	22.14 ± 0.0079	21.71 ± 0.0101	25.26 ± 0.0087	28.86 ± 0.0112	29.37 ± 0.0093	27.03 ± 0.0068
6	27.39 ± 0.0094	25.08 ± 0.0124	30.54 ± 0.0106	34.89 ± 0.0138	35.52 ± 0.0115	32.67 ± 0.0084
8	32.85 ± 0.0113	31.54 ± 0.0142	35.91 ± 0.0121	41.01 ± 0.0157	41.76 ± 0.0133	38.40 ± 0.0102
10	38.37 ± 0.0128	37.12 ± 0.0161	41.37 ± 0.0138	47.28 ± 0.0174	48.15 ± 0.0149	44.28 ± 0.0116
12	44.10 ± 0.0147	43.79 ± 0.0182	46.92 ± 0.0154	53.64 ± 0.0196	54.63 ± 0.0167	50.25 ± 0.0134
14	50.01 ± 0.0165	48.55 ± 0.0203	52.56 ± 0.0173	60.09 ± 0.0215	61.20 ± 0.0184	56.31 ± 0.0149
16	56.01 ± 0.0183	55.37 ± 0.0224	58.26 ± 0.0191	66.63 ± 0.0238	67.86 ± 0.0201	62.43 ± 0.0168
18	62.13 ± 0.0201	60.28 ± 0.0242	64.05 ± 0.0208	73.26 ± 0.0256	74.61 ± 0.0219	68.64 ± 0.0183
20	68.40 ± 0.0218	65.25 ± 0.0263	70.92 ± 0.0226	79.95 ± 0.0277	81.42 ± 0.0237	74.91 ± 0.0198

Journal of Molecular Science
Journal of Molecular Science
Volume 36 Issue 2, Year of Publication 2026, Page 647-660
DoI-10.004687/1000-9035.2026.075

22	74.79 ± 0.0237	69.34 ± 0.0281	76.89 ± 0.0244	86.77 ± 0.0295	88.39 ± 0.0255	81.29 ± 0.0216
24	81.30 ± 0.0254	74.46 ± 0.0302	84.89 ± 0.0262	93.64 ± 0.0318	95.38 ± 0.0273	87.74 ± 0.0231

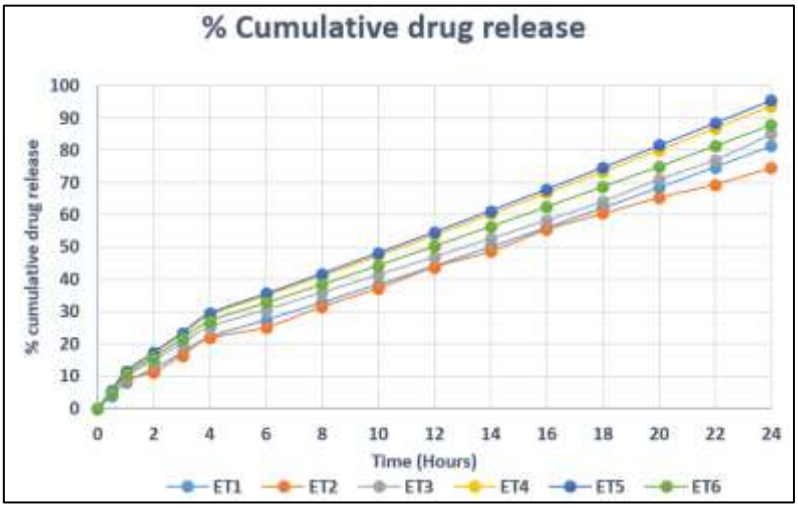

Figure 10: In vitro drug release of ET 1 to ET6

Table 14: In vitro drug release of ET 7 to ET13

Time (Hrs.)	ET7	ET8	ET9	ET10	ET11	ET12	ET13
0	0	0	0	0	0	0	0
0.5	6.24 ± 0.0023	5.37 ± 0.0015	4.77 ± 0.0028	5.13 ± 0.0019	5.13 ± 0.0031	5.34 ± 0.0022	4.65 ± 0.0014
1	11.79 ± 0.0042	10.89 ± 0.0031	9.69 ± 0.0048	10.44 ± 0.0035	10.44 ± 0.0053	10.83 ± 0.0039	9.42 ± 0.0027
2	17.67 ± 0.0065	16.53 ± 0.0048	14.70 ± 0.0072	15.84 ± 0.0054	15.84 ± 0.0079	16.44 ± 0.0058	14.28 ± 0.0041
3	23.91 ± 0.0087	22.26 ± 0.0066	19.80 ± 0.0094	21.33 ± 0.0071	21.33 ± 0.0102	22.14 ± 0.0077	19.23 ± 0.0056
4	30.45 ± 0.0111	28.05 ± 0.0085	24.96 ± 0.0118	26.88 ± 0.0093	26.88 ± 0.0127	27.90 ± 0.0098	24.24 ± 0.0072
6	36.48 ± 0.0136	33.90 ± 0.0104	30.18 ± 0.0145	32.49 ± 0.0115	32.52 ± 0.0151	33.72 ± 0.0119	29.31 ± 0.0088
8	42.54 ± 0.0158	39.84 ± 0.0123	35.49 ± 0.0171	38.19 ± 0.0134	38.25 ± 0.0178	39.63 ± 0.0142	34.47 ± 0.0105
10	48.75 ± 0.0182	45.93 ± 0.0144	40.89 ± 0.0197	44.04 ± 0.0156	44.10 ± 0.0203	45.69 ± 0.0165	39.72 ± 0.0121
12	55.14 ± 0.0205	52.11 ± 0.0163	46.38 ± 0.0221	49.95 ± 0.0177	50.04 ± 0.0228	51.82 ± 0.0184	45.06 ± 0.0138
14	61.68 ± 0.0229	58.38 ± 0.0185	51.96 ± 0.0246	55.95 ± 0.0198	56.07 ± 0.0253	58.03 ± 0.0207	50.49 ± 0.0156
16	68.40 ± 0.0254	64.71 ± 0.0206	57.60 ± 0.0272	62.04 ± 0.0221	62.16 ± 0.0278	64.30 ± 0.0228	55.98 ± 0.0172
18	75.36 ± 0.0278	71.16 ± 0.0228	63.33 ± 0.0297	68.22 ± 0.0243	68.32 ± 0.0304	70.72 ± 0.0251	61.56 ± 0.0189
20	82.59 ± 0.0301	77.67 ± 0.0249	69.12 ± 0.0321	74.46 ± 0.0265	74.50 ± 0.0329	77.20 ± 0.0273	67.20 ± 0.0206
22	89.91 ± 0.0325	84.27 ± 0.0271	75.04 ± 0.0346	80.73 ± 0.0288	80.89 ± 0.0355	83.80 ± 0.0296	72.96 ± 0.0224
24	97.38 ± 0.0349	90.93 ± 0.0294	80.98 ± 0.0371	87.12 ± 0.0312	87.31 ± 0.0381	90.43 ± 0.0318	78.75 ± 0.0242

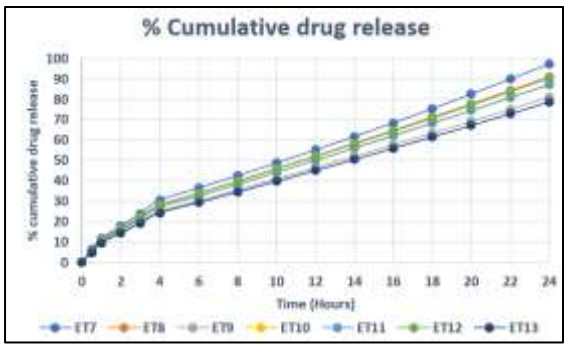

Fig 11: In vitro drug release of ET7 to ET13

A progressive rise in drug release over a 24-hour period was seen in the in vitro drug release analysis of formulations ET1–ET13, suggesting sustained-release behavior. The formulation with the greatest cumulative drug release was ET7 (97.38 ± 0.0349%), followed by ET5 (95.38 ± 0.0273%) and ET4 (93.64 ± 0.0318%). ET2 showed the least amount of drug release (74.46 ± 0.0302%). The dissolution data's high consistency and repeatability are shown by the low standard deviation values. ET7 might be regarded as the ideal formulation for further research as it showed the most effective drug release profile overall.

ANOVA for Quadratic model
Response 3: % Cumulative Drug Release

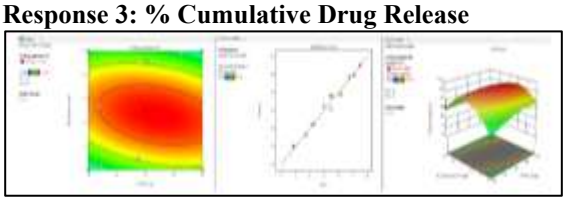

Figure 12: A) MCC vs. Crospovidone counterplot on percentage cumulative drug release; B) Predicted vs. Actual plot; and C) MCC vs. Crospovidone 3D surface plot on percentage cumulative drug release

Journal of Molecular Science
Journal of Molecular Science
Volume 36 Issue 2, Year of Publication 2026, Page 647-660
DoI-10.004687/1000-9035.2026.075

6.2.2.4 Stability study of proniosomal Tablet

Table 15: Stability study of Erlotinib Tablet

Formulation code	Stability parameter	Initial	1 month	2 month	3 month
ET7	**% Friability**	0.397 %	0.398 %	0.398 %	0.399 %
	Drug content (%)	95.59 ± 0.0147	95.52 ± 0.0318	94.47 ± 0.0608	94.43 ± 0.0511
	In vitro drug release	97.38 ± 0.0458	97.32 ± 0.00584	97.25 ± 0.0149	97.20 ± 0.0280

The stability investigation of the improved formulation ET7 exhibited good stability over a period of 3 months. Friability did not significantly vary, staying below 1%, suggesting acceptable mechanical strength. The in vitro drug release decreased somewhat from 97.38 ± 0.0458% to 97.20 ± 0.0280%, although the drug content only slightly decreased from 95.59 ± 0.0147% to 94.43 ± 0.0511%. These findings demonstrate that ET7 retained its physicochemical features and performance throughout storage, exhibiting excellent stability.

6.2.2.5 *In vivo* activity

Table 16: Change in Body weight

Group	Initial Body Weight (g)	Final Body Weight (g)	Change in Body Weight (%)
Normal Control	2850 ± 45	2971 ± 42	+4.25± 2.21
Tumor Control	2880 ± 38	2660 ± 35	−7.64± 1.72
Standard Drug (25mg)	2860 ± 36	2720 ± 37	-4.90± 1.76
ET (10mg)	2870 ± 39	2792 ± 36	−2.72± 1.82
ET (25mg)	2855 ± 42	2942 ± 38	+3.05± 2.02

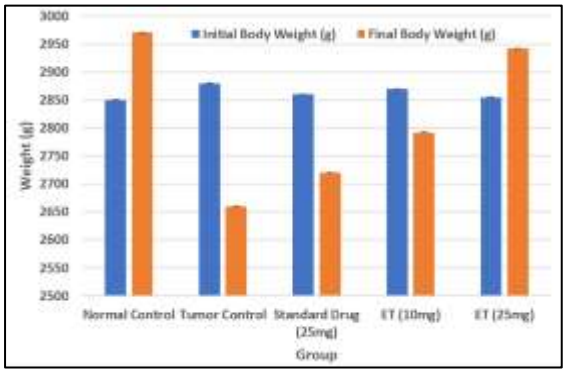

Figure 13: Effect of treatment on Body weight Changes

Table 17: Effect of Erlotinib & ET formulation on Tumor Volume

Group	Tumor Volume on Day 7 (cm^3)	Tumor Volume on Day 14 (cm^3)	Tumor Volume on Day 28 (cm^3)
Normal Control	0	0	0
Tumor Control	1.82 ± 0.09	3.94 ± 0.14	6.85 ± 0.21
Standard Drug (25mg)	1.81 ± 0.09	3.08 ± 0.12	4.76 ± 0.17
ET (10mg)	1.80 ± 0.08	2.42 ± 0.10	3.01 ± 0.13
ET (25mg)	1.06 ± 0.08	1.11 ± 0.10	1.48 ± 0.12

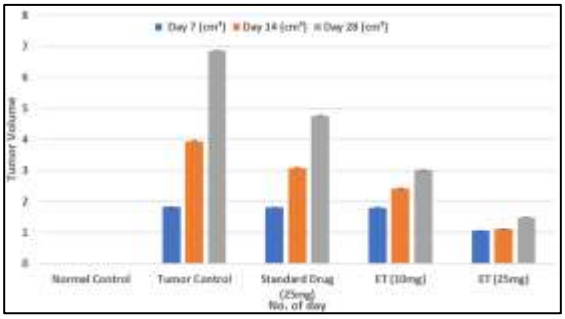

Figure 14: Effect of Erlotinib & ET formulation on Tumor Volume

Table 18: Effect of Erlotinib & ET formulation on Tumor Weight

Group	Tumor Weight (g)
Normal Control	0
Tumor Control	8.42 ± 0.31
Standard Drug (25mg)	5.88 ± 0.22
ET (10mg)	5.76 ± 0.19
ET (25mg)	3.14 ± 0.18

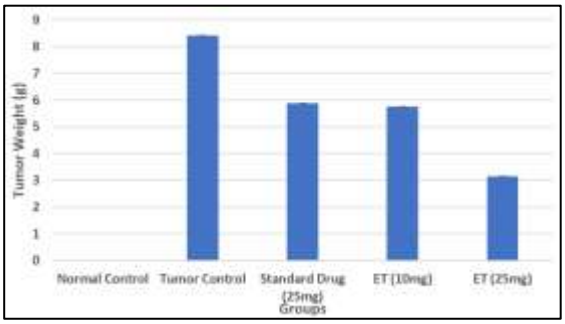

Figure 15: Effect of Erlotinib & ET formulation on Tumor Weight

Table 19: Effect of Erlotinib & ET formulation on Hematological Parameters

Group	Hemoglobin (g/dL)	RBC ($\times 10^6$ cells/mm^3)	WBC ($\times 10^3$ cells/mm^3)
Normal Control	13.8 ± 0.32	6.42 ± 0.21	7.15 ± 0.28
Tumor Control	9.6 ± 0.27	4.11 ± 0.18	12.84 ± 0.41
Standard Drug (25mg)	12.4 ± 0.30	5.88 ± 0.17	9.43 ± 0.32
ET (10mg)	11.2 ± 0.29	5.16 ± 0.16	10.38 ± 0.35
ET (25mg)	12.9 ± 0.30	6.05 ± 0.19	8.12 ± 0.33

Journal of Molecular Science
Journal of Molecular Science
Volume 36 Issue 2, Year of Publication 2026, Page 647-660
DoI-10.004687/1000-9035.2026.075

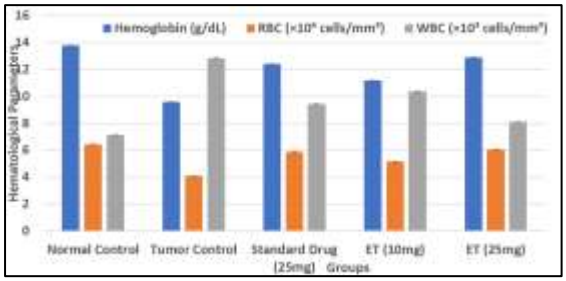

Figure 16: Effect of Erlotinib & ET formulation on Hematological Parameters

Table 20: Effect of Erlotinib & ET formulation on Liver Function Parameters

Group	ALT (U/L)	AST (U/L)	ALP (U/L)	Total Bilirubin (mg/dL)
Normal Control	32.4 ± 1.6	41.8 ± 1.9	96.5 ± 3.2	0.62 ± 0.03
Tumor Control	78.6 ± 2.8	96.4 ± 3.1	182.7 ± 5.4	1.84 ± 0.07
Standard Drug (25mg)	58.9 ± 2.3	75.6 ± 2.5	149.5 ± 4.6	1.31 ± 0.06
ET (10mg)	56.1 ± 1.8	66.8 ± 2.2	148.2 ± 3.9	1.15 ± 0.04
ET (25mg)	39.8 ± 1.9	49.2 ± 2.1	108.4 ± 3.6	0.79 ± 0.04

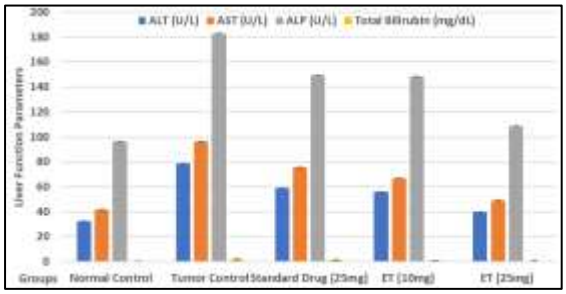

Figure 17: Effect of Erlotinib & ET formulation on Liver Function Parameters

Table 21: Effect of Erlotinib & ET formulation on Kidney Function Parameters

Group	Serum Creatinine (mg/dL)	Blood Urea Nitrogen (BUN) (mg/dL)	Serum Sodium (mEq/L)	Serum Potassium (mEq/L)
Normal Control	0.72 ± 0.03	18.4 ± 0.8	142.6 ± 2.4	4.3 ± 0.2
Tumor Control	1.84 ± 0.07	38.9 ± 1.4	128.5 ± 2.1	5.9 ± 0.3
Standard Drug (25mg)	1.41 ± 0.06	30.7 ± 1.1	133.2 ± 2.2	5.3 ± 0.2
Erlotinib (10mg)	0.98 ± 0.04	29.9 ± 0.9	134.1 ± 2.3	5.1 ± 0.1
Erlotinib (25mg)	0.88 ± 0.03	21.6 ± 0.8	139.8 ± 2.1	4.4 ± 0.2

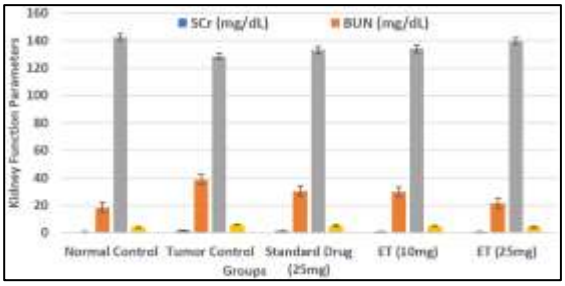

Figure 18: Effect of treatment on Kidney Function Parameters

Table 22: Effect of Erlotinib & ET formulation on Survival Parameters

Group	Mean Survival Time (Days)	% Increase in Life Span (%ILS)
Normal Control	—	100
Tumor Control	24.3 ± 1.1	10
Standard Drug (25mg)	38.4 ± 1.4	58.02
ET (10mg)	31.2 ± 1.2	28.40
ET (25mg)	41.8 ± 1.4	72.02

Values are expressed as Mean ± SEM (n = 6)

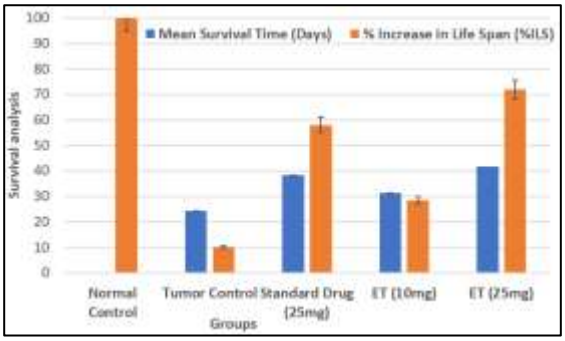

Figure 19: Effect of treatment on % increase in Life Span

Histopathology: -

1. Tumor

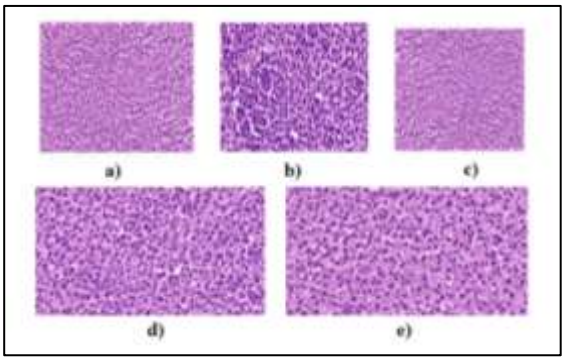

Figure 20: Tumor examination a) Normal control b) Tumor control c) Standard drug (25mg) d) ET 7-low dose (10mg) e) ET 7-high dose (25mg)

Tumor tissue: A histopathological analysis of the tumor control group's tumor tissue revealed necrotic areas, cellular atypia, and dense tumor cell proliferation, all of which indicated the tumor's progressive progression. Tumor cell density decreased and necrosis increased when the conventional medication and Erlotinib formulations

Journal of Molecular Science
Volume 36 Issue 2, Year of Publication 2026, Page 647-660
DoI-10.004687/1000-9035.2026.075

were administered. Compared to low-dose groups, ET high-dose treatment groups demonstrated a significant decrease in tumor development and improved restoration of tissue architecture.

2. Liver

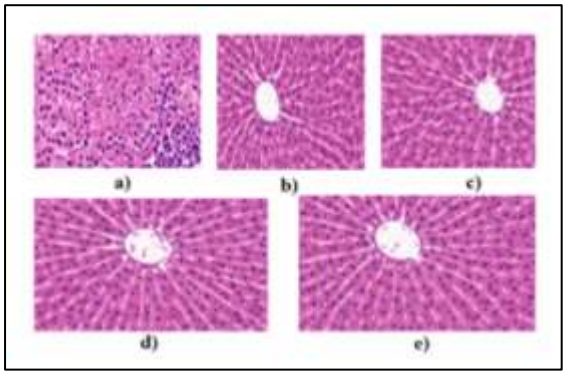

Figure 21: Liver examination a) Normal control b) Tumor control c) Standard drug (25mg) d) ET 7-low dose (10mg) e) ET 7-high dose (25mg)

Liver Tissue: Hepatocellular deterioration, congestion, and inflammatory infiltration were seen in liver slices from the tumor control group. Hepatic architecture is enhanced and cellular damage is decreased when the conventional medication and ET formulations are used. Hepatocyte organization was mostly normal in high-dose ET therapy groups, with very slight degenerative alterations.

3. Kidney

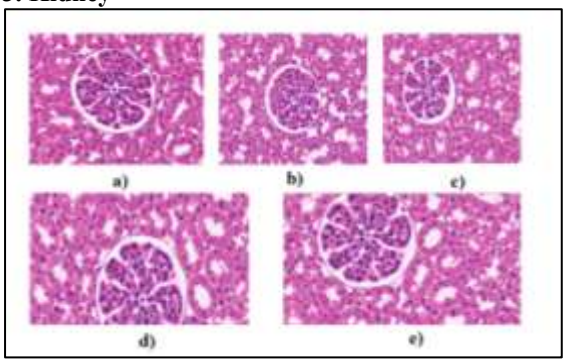

Figure 21: Kidney examination a) Normal control b) Tumor control c) Standard drug (25mg) d) ET 7-low dose (10mg) e) ET 7-high dose (25mg)

Kidney Tissue: The tumor control group's kidney tissue had glomerular injury, tubular degeneration, and inflammatory alterations. The renal architecture of the ET treatment groups improved, with less tube damage and glomerular structure preservation. When compared to ET low-dose groups, ET high-dose groups demonstrated superior kidney protection.

4. Spleen

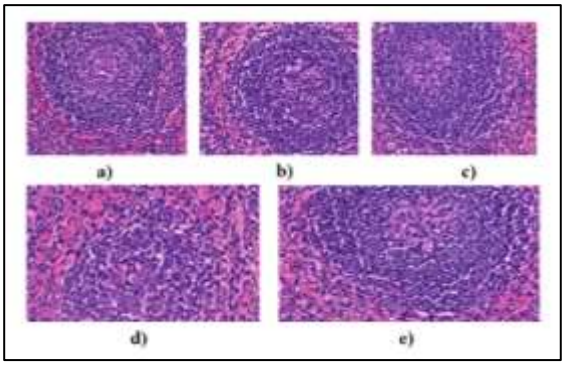

Figure 22: Spleen examination a) Normal control b) Tumor control c) Standard drug (25mg) d) ET 7-low dose (10mg) e) ET 7-high dose (25mg)

Spleen Tissue: The tumor control group's spleen sections showed lymphoid depletion, congestion, and altered splenic architecture. Treatment with the usual medication and ET restored splenic structure and decreased inflammatory alterations. White pulp and red pulp organization was almost normal in ET high-dose treatment groups.

7. CONCLUSION:

The current work used a Box-Behnken Design-based QbD technique to effectively produce and optimize proniosomal tablets loaded with erlotinib hydrochloride. While FTIR and SEM verified drug–excipient compatibility and effective vesicle formation, the improved proniosomal formulation (ER2) demonstrated high drug content, entrapment efficiency, nanosized particle size, and excellent stability. Under accelerated settings, the improved tablet formulation (ET7) showed stability, prolonged drug release, and acceptable tablet properties. Additionally, as compared to the tumor control group, in vivo trials demonstrated considerable reduction of tumor development, better hematological and biochemical parameters, longer life, and less systemic toxicity. More pharmacokinetic and clinical research is necessary since the proposed proniosomal tablet presents a potential oral delivery strategy for Erlotinib with improved therapeutic effectiveness and prolonged drug release.

8. DISCLOSURE STATEMENT

The authors declare no conflict of interest.

9. FUNDING

The authors received no funding for this work.

10. DECLARATION OF COMPETING INTEREST

Authors declare there are no conflict of interest.

11. REFERENCES

1. World Health Organization. WHO guidelines for safe surgery 2009: safe surgery saves lives. Geneva: World

Journal of Molecular Science
Volume 36 Issue 2, Year of Publication 2026, Page 647-660
DoI-10.004687/1000-9035.2026.075

Health Organization; 2009.
2. Panchal RR, Patange HS, Nimkar VS, Channawar MA, Bakde BV, Chandewar AV. Self-emulsifying drug delivery system: a novel approach in drug delivery: a review. Research Journal of Pharmaceutical Technology. 2012; 5(1):1-7.
3. Kaur P, Kaur L. Niosomes used as targeting drug delivery system: an overview. Asian J Res Chem. 2014; 7(7):687-692.
4. Walve JR, Bakliwal SR, Rane BR, Pawar SP. Transfersomes: a surrogate carrier for transdermal drug delivery system. International Journal of Applied Biology and Pharmaceutical Technology. 2011; 2(1):204-214.
5. Vale CA, Corvo ML, Martins LC, Marques CR, Storm G, Cruz ME, et al. Construction of enzymosomes: optimization of coupling parameters. In: NSTI Nanotech 2006. Vol. 2. Boston: NSTI; 2006. p. 396-397.
6. Kish-Trier E, Hill CP. Structural biology of the proteasome. Annual review of biophysics. 2013; 42:29-49.
7. Kaneda Y. Virosomes: evolution of the liposome as a targeted drug delivery system. Adv Drug Deliv Rev. 2000; 43(2-3):197-205.
8. Saraf S, Gupta D, Kaur CD, Saraf S. Sphingosomes: a novel approach to vesicular drug delivery. Int J Curr Sci Res. 2011; 1(2):63-68.
9. 9. González-Paredes A, Manconi M, Caddeo C, Ramos-Cormenzana A, Monteoliva-Sánchez M, Fadda AM. Archaeosomes as carriers for topical delivery of betamethasone dipropionate: in vitro skin permeation study. Journal of liposome research. 2010; 20(4):269-276.
10. Subodh D, Amit J, Mehta SC, Gupta P, Jain S, Sahu J. Niosomes: the ultimate drug carrier. Drug Invent Today. 2010; 2(1):72-81.
11. Ramadan WM, Singh AP. Preparation of acyclovir loaded nonionic surfactant vesicles (niosomes) using reverse phase evaporation technique. Research Journal of Pharmacy and Technology. 2009; 2(4):793-795.
12. Srikanth K, Nappinnai M, Gupta VR. Proniosomes: a novel drug carrier system. Research Journal of Pharmacy and Technology. 2010; 3(3):709-711.
13. Kondawar MS, Kamble KG, Malusare MK, Waghmare JJ, Shah ND. Proniosome-based drug delivery system for clotrimazole. Research Journal of Pharmacy and Technology. 2011; 4(8):1284-1287.
14. Nasr M. In vitro and in vivo evaluation of proniosomes containing celecoxib for oral administration. AAPS PharmSciTech. 2010; 11(1):85-89.
15. Khatoon M, Shah KU, Din FU, Shah SU, Rehman AU, Dilawar N, et al. Proniosomes derived niosomes: recent advancements in drug delivery and targeting. Drug Delivery. 2017; 24(2):56-69.
16. Zingade SG, Nagoba SN, Swami AB, Swamy SMV. Formulation and evaluation of liposomes containing erlotinib hydrochloride. Bull Environ Pharmacol Life Sci. 2022; 11(4):1-8.
17. Shehata TM, Abdallah MH, Ibrahim MM. Proniosomal oral tablets for controlled delivery and enhanced pharmacokinetic properties of acemetacin. AAPS PharmSciTech. 2015; 16(2):375-383.
18. Allen TM, Mehra T, Hansen C, Chin YC. Stealth liposomes: an improved sustained release system for 1-β-D-arabinofuranosylcytosine. Cancer Research. 1992; 52(9):2431-2439.
19. Gabizon A, Catane R, Uziely B, Kaufman B, Safra T, Cohen R, et al. Prolonged circulation time and enhanced accumulation in malignant exudates of doxorubicin encapsulated in polyethylene glycol-coated liposomes. Cancer Research. 1994; 54(4):987-992.
20. Perrett S, Golding M, Williams WP. A simple method for the preparation of liposomes for pharmaceutical applications: characterization of the liposomes. Journal of pharmacy and pharmacology. 1991; 43(3):154-161.
21. Kashid VA, Ghugarkar PG, Jesupillai M, Ahire SB. Formulation and evaluation of proniosomes loaded with captopril maltodextrin. African Journal of Biological Sciences. 2024; 6(Suppl 2).
22. Shah D, Shah Y, Pradhan R. Development and evaluation of controlled-release diltiazem HCl microparticles using cross-linked poly (vinyl alcohol). Drug development and industrial pharmacy. 1997; 23(6):567-574.
23. Nikam VI, Maniyar SI. Formulation development and evaluation of niosomal gel of collective antifungal agents. Asian Journal Pharm Clinical Research. 2022; 15(2):64-74.
24. Kumar R, Patil MB, Patil SR, Paschapur MS. Formulation and evaluation of effervescent floating tablet of famotidine. Int J PharmTech Res. 2009; 1(3):754-763.
25. Chauhan I, Yasir M, Verma M, Singh AP. Nanostructured lipid carriers: a groundbreaking approach for transdermal drug delivery. Advanced pharmaceutical bulletin. 2020; 10(2):150-165.
26. Mokale VJ, Patil HI, Patil AP, Shirude PR, Naik JB. Formulation and optimisation of famotidine proniosomes: an *in vitro* and *ex vivo* study. Journal of Experimental Nanoscience. 2016; 11(2):97-110.
27. Reza MS, Quadir MA, Haider SS. Comparative evaluation of plastic, hydrophobic and hydrophilic polymers as matrices for controlled-release drug delivery. J Pharm Pharm Sci. 2003; 6(2):282-291.
28. Erdoğar N. Development of oral tablet formulation containing erlotinib: randomly methylated-β-cyclodextrin inclusion complex using direct compression method. Turkish Journal of Pharmaceutical Sciences. 2021; 18(5):589-597.
29. Patel S, Kaushal AM, Bansal AK. Compression physics in the formulation development of tablets. Crit Rev Therapeutic Drug Carrier System. 2006; 23(1):1-65.
30. Sokač K, Miloloža M, Kučić Grgić D, Žižek K. Polymeric amorphous solid dispersions of dasatinib: formulation and ecotoxicological assessment. Pharmaceutics. 2024; 16(4):551.
31. Dharani S, Mohamed EM, Khuroo T, Rahman Z, Khan MA. Formulation characterization and pharmacokinetic evaluation of amorphous solid dispersions of dasatinib. Pharmaceutics. 2022; 14(11):2450.
32. Dhobale A, Mahale A, Shirsat M, Joshi D, Dhembre G, Thakare M. Design, development and characterization of losartan potassium sustained-release matrix tablet. World J Pharm Pharm Sci. 2018; 7:1349-1362.
33. Pascale F, Pelage JP, Wassef M, Ghegediban SH, Saint-Maurice JP, De Baere T, et al. Rabbit VX2 liver tumor model: a review of clinical, biology, histology, and tumor microenvironment characteristics. Frontiers in oncology. 2022; 12:871829.
34. Reitman S, Frankel S. A colorimetric method for the determination of serum glutamic oxalacetic and glutamic pyruvic transaminases. Am J Clin Pathol. 1957; 28(1):56-63.
35. Zhou HZ, Wang DX, Qian YQ, Wei JQ, Ma S, Feng YJ, et al. Large animal models for investigating the applications of photodynamic therapy. Zoological Research. 2025; 46(3):551-566.
36. Bancroft JD, Gamble M, editors. Theory and practice of histological techniques. 6th edition. Philadelphia: Elsevier Health Sciences; 2008.